The Strangeness and Charm of Dense Nuclear Matter

Peter Senger
Gesellschaft für Schwerionenforschung (GSI)
Postfach 110552, D-64220 Darmstadt, Germany

May 8, 2002

Abstract

The creation of strangeness and charm in nucleus-nucleus collisions at threshold beam energies is discussed as a probe for compressed baryonic matter. Experimental data on strangeness production at SIS energies indicate that the properties of kaons and antikaons are modified in dense nuclear matter. The yield of K^+ mesons emitted in heavy-ion collisions at beam energies below 1.5 AGeV is found to be sensitive to the nuclear equation-of-state. An experiment is proposed at the future GSI facility to explore the QCD phase diagram in the region of highest baryon densities. This approach is complementary to the studies of matter at high temperatures performed at the CERN-SPS, RHIC and the future LHC. Experimental observables and the proposed detector system will be discussed.

1 Introduction

The goal of the nuclear reaction program at the present and the future GSI accelerators is to investigate the properties of highly compressed nuclear matter. Such a form of matter exists in various so far unexplored phases in the interior of neutron stars and in the core of supernova explosions. The relevant degrees of freedom of dense baryonic matter are not obvious. There is no reliable prediction for a critical baryon density at which hadrons (at zero temperature) dissolve into quarks and gluons and how the properties of the particles are modified in the different phases of strongly interacting matter. These questions are related to puzzling features of QCD such as confinement and chiral symmetry breaking. Experimental efforts at heavy ion accelerators are performed worldwide in order to obtain information on nuclear matter under extreme conditions.

2 Strange mesons in dense baryonic matter

Strange mesons are regarded as promising probes both for the study of the in-medium properties of hadrons and the nuclear equation-of-state. According to various calculations, the properties of kaons and antikaons are modified in dense baryonic matter (see e.g. [1, 2, 4]). In mean-field calculations, this effect is caused by a repulsive K^+N potential and an attractive K^-N potential. It has been speculated [3] that an attractive K^-N potential will lead to Bose condensation of K^- mesons in the core of neutron stars above baryon densities of about 3 times saturation density. Microscopic calculations predict a dynamical broadening of the K^- meson spectral function which is shifted towards smaller energies [5, 6]. This effect enhances significantly the in-medium cross section for the strangeness exchange reaction πY $\rightarrow$ K^-N (with Y = Λ, Σ) and thus the K^- yield.

Experiments on kaon and antikaon production and propagation in heavy-ion collisions at relativistic energies have been performed with the Kaon Spectrometer and the FOPI detector at the heavy-ion synchrotron SIS at GSI Darmstadt. Recent results are published in [7, 8, 9, 10, 11, 12].

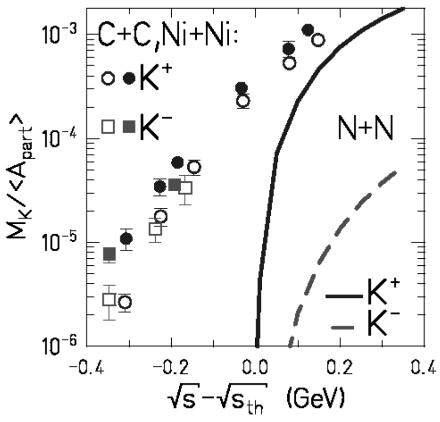

Figure 1: K^+ (circles) and antikaon (squares) multiplicity per participating nucleon as a function of the Q-value for C+C (open symbols) and Ni+Ni (full symbols) collisions [9, 11, 13]. The lines correspond to parameterizations of the production cross sections for K^+ (solid) and K^- (dashed) in nucleon-nucleon collisions [14, 15, 16].

In order to illustrate in-medium effects on K^+ and K^- production we compare nucleus-nucleus to proton-proton collisions. Fig. 1 shows the multiplicity of K^+ and K^- mesons per average number of participating nucleons $M_K/ < A_{part} >$ as function of the Q-value in the NN system. The data were measured in C+C and Ni+Ni collisions by the KaoS Collaboration [9, 11, 13]. The lines represent parameterizations of the available proton-proton data averaged over the isospin channels [14, 15, 16]. In "nucleon-nucleon" collisions the K^+ multiplicity exceeds the K^- multiplicity by 1-2 orders of magnitudes at the same Q-value. This large difference has disappeared for nucleus-nucleus collisions where the kaon and antikaon data nearly fall on the same curve. This observation demonstrates that in nucleus-nucleus collisions the production of antikaons is much more enhanced than the production of kaons. Within transport calculations, the K$^-$ yield enhancement is explained by two effects: (i) strangeness exchange reactions such as $\pi\Lambda \rightarrow$K$^-$N and (ii) a reduced effective K$^-$ mass in dense nuclear matter [4].

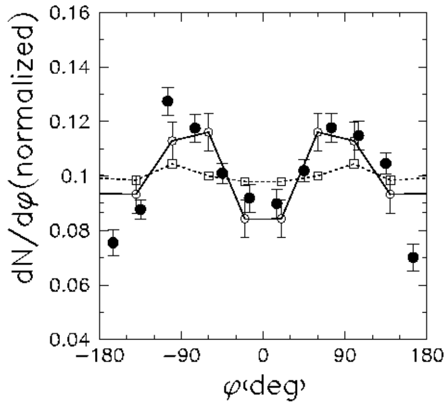

Figure 2: K$^+$ azimuthal angle distribution for semi-central Au+Au collisions at 1 AGeV. The data (full dots) are measured in the rapidity range 0.2 $\leq y/y_{proj} \leq$ 0.8 [8]. The open symbols and the lines respresent results of a QMD transport calculation [18] with repulsive K$^+$N potential (open circles, full line) and without K$^+$N potential (open squares, dashed line).

Another observable consequence of in-medium KN potentials is their influence on the propagation of kaons and antikaons in heavy-ion collisions. The measured azimuthal emission patterns of K^+ mesons $-$ which cannot be absorbed as they contain an antistrange quark $-$ contradict the naive picture of a long mean free path in nuclear matter. The particular feature of sideward flow [10] and the pronounced out-of-plane emission around midrapidity [8] indicate that K^+ mesons are repelled from the regions of increased baryonic density as expected for a repulsive K^+N potential [17, 18]. The azimuthal angle distribution of K^+ mesons from Au+Au collisions at a beam energy of 1 AGeV is shown in figure 2. The data (full symbols) [8] are compared to results of a QMD transport calculation with (open circles) and without (open squares) in-medium effects [18]. Clearly the data support the calculation which assumes a repulsive K^+N potential.

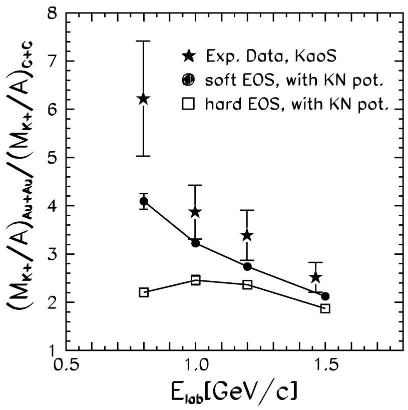

Figure 3: K$^+$ ratio measured in inclusive Au+Au and C+C collisions as function of beam energy (stars) [12]. The data are compared to QMD calculations assuming nuclear compressibilities of κ = 200 MeV (full dots) and 380 MeV (open squares) [19].

The yield of kaons observed in heavy-ion collisions is not only sensitive to the kaon in-medium properties but also to the compressibility of nuclear matter. The two effects can be disentangled by measuring the K^+ production excitation function in a very heavy system and - as a reference system - in a very light collision system. Figure 3 shows the ratio of the K^* multiplicities measured in Au+Au and C+C collision as function of beam energy [12]. The comparison of the data to the results of QMD transport calculations assuming different values for the nuclear compressibility provides evidence for a soft nuclear equation of state [19].

3 Future experiments at high baryon densities

Experiments at the CERN-SPS have studied high-energy heavy-ion collisions in order to explore the QCD phase diagram in the region of high temperatures and low baryon densities. In nature such extreme conditions were reached in the early universe, a few microseconds after the big bang. Experiments at RHIC and at the future LHC will continue this way and investigate the quark-gluon plasma at vanishing net baryon density (see figure 4).

The major goal of the nuclear reaction experiment at the future GSI facility is to explore the presently almost unknown region of high baryon densities in the phase diagram of strongly interacting matter. The territory of dense baryonic matter accessible in heavy-ion collisions is located between the line of chemical freeze-out and the hadron/parton phase boundary, as indicated by the hatched area in figure 4. Moreover, new states of matter beyond the deconfinement and chiral transition at high net baryon densities and moderate temperatures may be within the reach of the experiment. A particular challenge for future heavy-ion experiments is the search for the predicted "critical point" in the phase diagram of strongly interacting matter. Pioneering experiments which investigated hadronic observables in the energy range from 2 to about 15 AGeV have been performed at the AGS in Brookhaven.

Figure 4 presents a calculated chemical freeze-out curve and the freeze-out points (full dots) as derived from particle production data obtained at SIS, AGS, SPS and RHIC [20, 21, 22, 23]. The baryon density at freeze-out corresponds to a value of 0.75 ρ_0. The curve labeled "Lattice QCD" represents the phase boundary as predicted by a recent QCD lattice calculation for finite baryon chemical potential [24]. According to the calculations, the phase boundary and the freeze-out curve merge at small baryon chemical potentials ($\mu_B \leq$ 200-300 MeV). The SPS and RHIC data suggest that - at ultra-relativistic beam energies - hadronization and freeze-out occurs almost simultaneously (which implies that the fireball was born into the quark-gluon phase).

The QCD lattice calculation predicts a critical point which is located close to the AGS freeze-out point and hence could be reached with the future GSI accelerator. The discovery of the critical point would represent a major progress in the exploration of the QCD phase diagram [25].

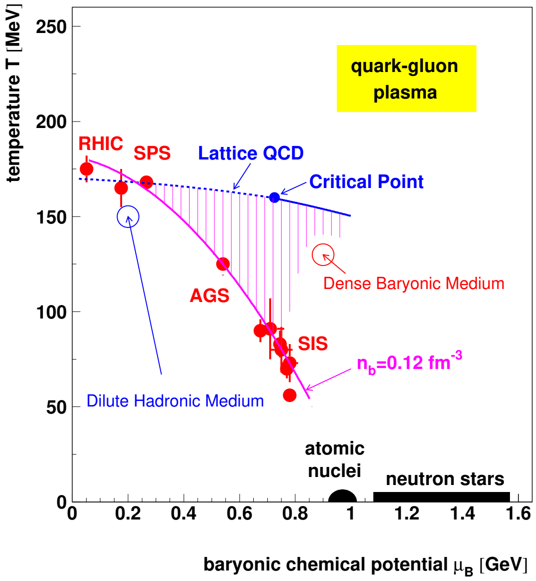

Figure 4: The phase diagram of strongly interacting matter. The symbols represent freeze-out points obtained with a statistical model analysis from particle ratios measured in heavy collisions [21, 20, 22]. The curve through the data points refers to a calculation of the chemical freeze-out which occurs at a constant baryon density of $\rho_B = 0.75\ \rho_0$ (with $\rho_0 = 0.16$ fm^{-3}). The curve labeled "Lattice QCD" represents the phase boundary as obtained with a QCD lattice calculation [24] with a critical point (full dot) at T=160±3.5 MeV and $\mu_B =$ 725±35 MeV ($\rho_B \approx 3\ \rho_0$). In the region of the circle labeled "dilute hadronic medium" the baryon density is ρ_B=0.038 fm^{-3} $\approx 0.24\ \rho_0$. The corresponding value for the other circle ("dense baryonic medium") is ρ_B=1.0 fm^{-3} ≈ 6.2 ρ_0. The hatched area marks the region of equilibrated matter at high baryon densities.

The envisaged physics program at the future facility includes:

- search for signatures of chiral symmetry restoration in dense baryonic matter. Probes: Dilepton pairs from light vector mesons, the yield of open charm (D mesons) and the ratio of open to hidden charm.
- search for signatures of the deconfinement phase transition at large baryonic chemical potentials. Probes: charmonium, strangeness, collective flow.
- search for the critical point. Probes: event-by-event fluctuations of hadronic observables (K/π ratio, average transverse momentum of hadrons)

- search for exotic states of matter such as condensates of strange particles or color superconductivity. Probes: strange and multistrange particles, K/π ratio

The (partial) restoration of chiral symmetry is expected to modify the in-medium spectral function of short lived vector mesons like the ρ-meson. This effect is studied experimentally by measuring the decay of a ρ-meson into a pair of leptons which are not disturbed by interaction with the fireball matter. An enhanced yield of electron-positron pairs in the low mass region of the invariant mass spectrum has been observed in central lead-lead collisions at 158 AGeV [31] and, recently, also at 40 AGeV [32]. It is still under debate whether this enhancement is caused by a shift and/or a broadening of the ρ-meson spectral function or by thermal radiation from the quark-gluon plasma [33] The actual error bars of the data are too large in order to clarify the situation.

No dilepton experiment has been performed so far in the beam energy range between 2 and 40 AGeV. We propose to measure the leptonic decay of light vector mesons (ρ-, ω- and ϕ mesons) in this beam energy range. These data will shed light on the fundamental question to what extend chiral symmetry is restored at high baryon densities and how this affects hadron masses. The

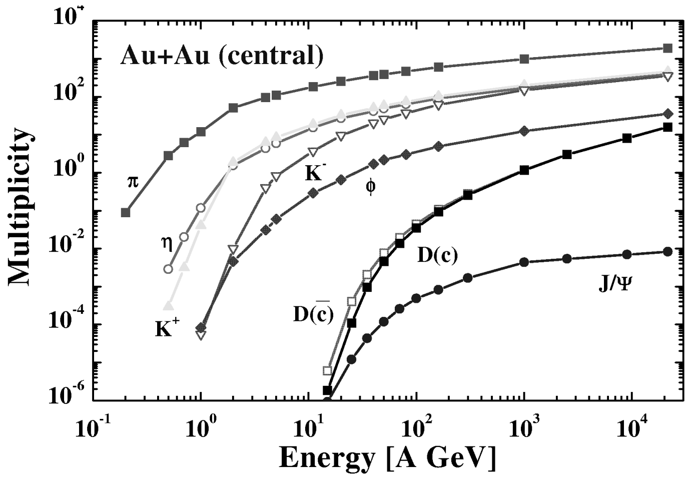

Figure 5: Multiplicities of mesons produced in central Au+Au collisions as function of beam energy according to the HSD transport code [30]

observation of mesons containing charm quarks is of particular importance. Due to the large mass of charm quarks, a charm-anticharm pair is expected to be produced predominantly in hard collisions between two quarks or two gluons. Hence charmed mesons are messengers from the early fireball - created prior to expansion and freezeout. For central lead-lead collisions an anomalous suppression of J/ψ mesons has been observed at SPS energies [26]. This effect was predicted and interpreted as screening of $c\bar{c}$ pairs in the quark phase [27].

Most of the created charm quarks, however, are confined in D-mesons together with a light quark. Therefore, the observation of open charm in heavy ion collisions is of crucial importance for the interpretation of signatures of a possible deconfinement phase transition. So far D mesons have not been observed in nucleus-nucleus collisions.

Charm production (both J/ψ and D mesons) will be also an important probe for the high baryon density regime of the QCD phase diagram. In particular at beam energies close to threshold, charm production might depend on the conditions inside the dense fireball. The charmonium yield − measured as function of collision centrality − will be sensitive to a possible deconfinement phase transition. The measurement of open charm provides the unique possibility to study in-medium properties of hadrons at very high baryonic densities. The effective masses of D-mesons - which consist of a heavy charm quark and a light quark - are expected to be modified substantially in dense matter, in a way analogous to the masses of K mesons [28, 29]).

The production thresholds in proton-proton (or proton-neutron) collisions are 11.3 GeV for J/ψ mesons, 11.9 GeV for D mesons and 14.9 GeV for Anti-D-mesons. Figure 5 shows multiplicities of J/ψ, D mesons and lighter mesons produced in central Au+Au collisions as function of beam energy as calculated with the HSD transport model [30].

A simultaneous measurement of charmonium, D mesons, multistrange hyperons and light vector mesons (together with protons, pions and kaons) in one single experiment has not been performed up to now. Such an experiment permits to study the behavior of different probes and their correlations under identical experimental conditions (such as impact parameter selection). An intriguing idea is to investigate collisions between deformed uranium nuclei and to select those events where the two nuclei collided tip-on-tip. In such a collision the baryonic density is increased by about 30 % (with respect to a collision between two spherical nuclei) and the reaction time is extended by almost a factor of 2 [34].

4 The Compressed Baryonic Matter (CBM) experiment

The planned experimental setup will be able to measure the observables discussed above in nucleus-nucleus collisions at beam energies between 2 and 40 AGeV. The energy range from 2 to 7 AGeV will be covered by the (slightly modified) HADES detector whereas the new "Compressed Baryonic Matter" (CBM) experiment is designed for the energy range from 7 to 40 AGeV.

The CBM detector is a universal instrument for the measurement of both leptons and hadrons and for the efficient identification of rare probes in a large background of charged particles. The experimental challenge is the large track density of charged particles in central Au+Au collisions at 25 AGeV. According to the URQMD event generator [35] such an event consists of about 160 protons, 800 charged pions and 60 kaons (K^+ and K^-). Based on these simulations we have designed the experimental setup. It turns out that the apparatus described below accepts about 80% of the protons, 60% of the kaons (including decay in flight), 67 % of the pions, 20% of J/ψ mesons and 30 % of the D mesons (branching ratios for the decays $J/\psi \rightarrow e^+e^-$ and $D \rightarrow K\ \pi\pi$ not included).

The experiment combines state-of-the-art detector components which in part are under development for future experiments at the Large Hadron Collider at CERN: large arrays of radiation hard silicon pixel (and strip) detectors for precise tracking and vertex reconstruction, transition radiation detectors and ring-imaging Cherenkov detectors for electron identification and resistive-plate-chamber arrays for time-of-flight measurements.

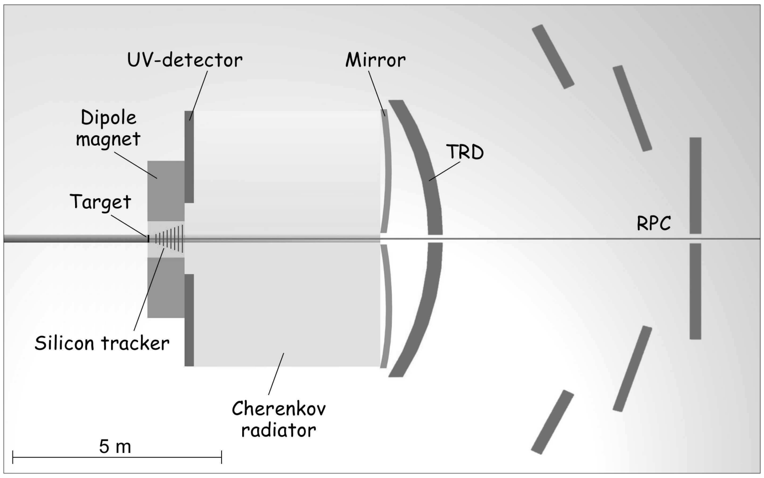

Figure 6: Sketch of the experimental setup (see text)

The proposed experimental setup (see figure 6) consists of the following components:

- Dipole magnet

  The magnetic field bends the particles according to their momentum (and charge) and prevents most of the abundantly produced δ-electrons from hitting the detectors.

- Radiation hard Silicon pixel/strip detectors

  A set of Silicon pixel (and strip) detectors close to the target allow to determine the particle trajectory (and hence the momentum) with high accuracy. This Silicon tracker will measure the decay topology of hyperons and hence their invariant mass. A vertex resolution of better than 50 μm is required for the identification of charmed mesons via their displaced decay vertex.

- Ring imaging Cherenkov detector (RICH)

  The RICH detector provides identification of electrons with $\gamma > 40$ corresponding to the momentum range of di-electrons from decaying ρ-mesons. When using a radiator with higher refractive index the RICH signals can be used to identify high energy pions and kaons. The main components of the RICH are the Cherenkov radiator, the mirror and the UV detector (see figure 6.

- Transition radiation detector (TRD)

  The TRD allows to identify high energy electrons ($\gamma > 2000$) and hence the measurement of charmonium via the invariant mass of the electron positron pair.

- TOF stop wall: resistive plate chambers (RPC)

  The large area RPC provides the stop signal for the time-of-flight measurement which allows the identification of low momentum particles. A TOF distance of 10 m results in a time difference of 400 ps for pions and kaons of 3 GeV/c momentum.

- TOF start detector (not shown in figure 6)

  A Diamond pixel detector provides the start signal for the TOF measurement. It will count directly the beam particles up to intensities of 10^9 ions/sec.

The Compressed Baryonic Matter (CBM) experiment is part of a proposal for a new accelerator facility at GSI in Darmstadt (see http://www.gsi.de/GSI-Future/cdr/).

5 Acknowledgement

The data on strangeness production presented in this paper were measured and analyzed by my colleagues of the KaoS Collaboration: I. Böttcher, A. Förster, E. Grosse, P. Koczoń, B. Kohlmeyer, M. Menzel, L. Naumann, H. Oeschler, E. Schwab, W. Scheinast, Y. Shin, H. Ströbele, C. Sturm, F. Uhlig, A. Wagner and W. Waluś. The conceptual design study of the compressed baryon matter experiment is performed by a working group which actually consists of A. Andronic, P. Braun-Munzinger, C. Finck, B. Friman, N. Herrmann, R. Holzmann, W. König, M. Lutz, P. S., Y. Shin, R. Simon, H. Ströbele and J. Stroth.

References

[1] G.E. Brown et al., Phys. Rev. **C 43** (1991) 1881

[2] J. Schaffner-Bielich et al., Nucl. Phys. **A 625** (1997) 325

[3] G.Q. Li, C.H. Lee and G.E. Brown, Phys. Rev. Lett. **79** (1997) 5214

[4] W. Cassing and E. Bratkovskaya, Phys. Rep. **308** (1999) 65

[5] T. Waas, N. Kaiser and W. Weise, Phys. Lett. **B 379** (1996) 34

[6] M. Lutz, Phys. Lett. **B 426** (1998) 12

[7] D. Best et al., Nucl. Phys. **A 625** (1997) 307

[8] Y. Shin et al., Phys. Rev. Lett. **81** (1998) 1576

[9] F. Laue, C. Sturm et al., Phys. Rev. Lett. **82** (1999) 1640

[10] P. Crochet et al., Phys. Lett. **B 486** (2000) 6

[11] M. Menzel et al., Phys. Lett. **B 495** (2000) 26

[12] C. Sturm et al., Phys. Rev. Lett. **86** (2001) 39

[13] R. Barth et al., Phys. Rev. Lett. **78** (1997) 4007

[14] A. Sibirtsev, Phys. Lett. **B 359** (1995) 29

[15] E.Bratkovskaya, W.Cassing and U.Mosel, Nucl. Phys. **A 622** (1997) 593

[16] A. Sibirtsev, W. Cassing and C.M. Ko, Z. Phys. **A 358** (1997) 101

[17] G.Q. Li, C.M. Ko, G.E. Brown, Phys. Lett. **B 381** (1996) 17

[18] Z.S. Wang et al., Eur. Phys. J. **A 5** (1999) 275

[19] C. Fuchs et al., Phys. Rev. Lett. **86** (2001) 1974

[20] R. Stock, Phys. Lett. B 456 (1999) 277

[21] P. Braun-Munzinger, I. Heppe, J. Stachel, Phys. Lett. B 465 (1999) 15

[22] J. Cleymans and K. Redlich, Phys. Rev. Lett. 81 (1998) 5284

[23] P. Braun-Munzinger, Nucl. Phys. A 681 (2001) 119c

[24] Z. Fodor and S. D. Katz, hep-lat/0106002

[25] K. Rajagopal, Nucl. Phys. A 661 (1999) 150c

[26] M. Abreu et al., Phys. Lett. **B 477** (2000) 28

[27] T. Matsui and H. Satz, Phys. Lett. **B 178** (1986) 416

[28] W. Weise et al. Proc. of the workshop "Hadrons in Matter", Hirschegg/Austria 2001

[29] A. Sibirtsev, K. Tsushima, A.W. Thomas, Eur. Phys. J. **A 6** (1999) 351

[30] W. Cassing, E. Bratkovskaya, A. Sibirtsev, nucl-th/0010071

[31] G. Agakichiev et al., Phys. Lett. **B 422** (1998) 405

[32] S. Damjanovic and K. Filimonov, nucl-ex/0109017

[33] R. Rapp, Nucl. Phys. **A 661** (1999) 33c

[34] Bao-An Li, Phys. Rev. **C 61** (2000) 021903

[35] S.A. Bass et al., Prog. Part. Nucl. Phys. **41** (1998) 225